Journal of Zhejiang University-SCIENCE A (Applied Physics & Engineering)
ISSN 1673-565X (Print); ISSN 1862-1775 (Online)
www.jzus.zju.edu.cn; link.springer.com
E-mail: jzus_a@zju.edu.cn

Numerical analysis of column collapse by smoothed particle hydrodynamics with an advanced critical state-based model*

Zhuang JIN[1,2], Zhao LU[†‡3,4], Yi YANG[5]

[1]*Department of Ocean Science and Engineering, Southern University of Science and Technology, Shenzhen 518055, China*
[2]*Southern Marine Science and Engineering Guangdong Laboratory (Guangzhou), Guangzhou 511458, China*
[3]*Civil and Environmental Engineering, University of Macau, Taipa, Macau, China*
[4]*Research and Development Center, Shenzhen Foundation Engineering Co. LTD, Shenzhen 518000, China*
[5]*Department of Civil Engineering, Chu Hai College of Higher Education, Tuen Mun, Hong Kong, China*
[†]E-mail: messi.luzhao@connect.umac.mo; yb87402@um.edu.mo

Received Dec. 16, 2020; Revision accepted Jan. 14, 2021; Crosschecked Oct. 20, 2021

Abstract: The complex behavior of granular material considering large deformation and post-failure is of great interest in the geotechnical field. Numerical prediction of these phenomena could provide useful insights for engineering design and practice. In this paper, we propose a novel numerical approach to study soil collapse involving large deformation. The approach combines a recently developed critical state-based sand model SIMSAND for describing complex sand mechanical behaviors, and the smoothed particle hydrodynamics (SPH) method for dealing with large deformation. To show the high efficiency and accuracy of the proposed approach, a series of column collapses using discrete element method (DEM) and considering the influence of particle shapes (i.e. spherical shape (SS), tetrahedral shape (TS), and elongated shape (ES)) were adopted as benchmarks and simulated by the proposed method. The parameters of SIMSAND were calibrated from the results of DEM triaxial tests on the same samples. Compared with the results of DEM simulations and reference solutions derived by published collapse experiments, the runout distance and final height of specimens with different particle shapes simulated by SPH-SIMSAND were well characterized and incurred a lower computational cost. Comparisons showed that the novel SPH-SIMSAND approach is highly efficient and accurate for simulating collapse, and can be a useful numerical analytical tool for real scale engineering problems.

Key words: Granular material; Smoothed particle hydrodynamics (SPH); Large deformations; Critical state; Collapse
https://doi.org/10.1631/jzus.A2000598 **CLC number:** TU434

1 Introduction

In some industry sectors, such as material handling, the economy and efficiency of the work depend to a large extent on the rational design of the relevant industrial facilities, which in turn depends on a deep knowledge of the properties of granular materials. The study of the mechanical properties of granular materials, in addition to having a great impact on industry, is of great significance in the context of natural disasters caused by the disruption of particle flows, such as debris, internal erosion (Yang et al., 2019a, 2019b, 2019c, 2020), and landslides (Jin et al., 2020; Yuan et al., 2020).

Having a comprehensive understanding of the mechanical behaviour of granular materials in collapse motion can provide better guidance and service in disaster prevention and engineering construction. Since the scale of damage caused by granular materials in nature is generally large, it is clearly impractical to conduct full-scale tests or numerical simulations.

‡ Corresponding author
* Project supported by the Shenzhen Research and Technology Fund (No. JSGG20180504170449754) and the grant from the Research Grants Council of the Hong Kong Special Administrative Region (No. UGC/FDS13/E06/18), China
ORCID: Zhuang JIN, https://orcid.org/0000-0001-6463-1379

Therefore, two kinds of model tests have been conducted: 2D rectangular channel flowing tests (Balmforth and Kerswell, 2005; Lajeunesse et al., 2005; Lube et al., 2005, 2007; Bui et al., 2008; Crosta et al., 2009) and 3D axisymmetric column flowing tests (Daerr and Douady, 1999; Lajeunesse et al., 2004; Lube et al., 2004). The experimental results of Lajeunesse et al. (2004, 2005) and Lube et al. (2004, 2005, 2007) inferred that the final deposition morphology (deposition radius, deposition height, and collapse rate) depends mainly on the initial aspect ratio of the granular sample.

To study the collapse process of granular materials in more detail, many scholars began to use numerical simulation methods to reproduce the indoor physical collapse test (Zhang et al., 2013, 2014, 2015; Dávalos et al., 2015; Fern and Soga, 2016; Wu et al., 2019; Yuan et al., 2019; Xiong et al., 2021). Generally, the methods could be classified in two main groups: discrete methods and continuum methods, both of which have their own advantages and drawbacks (Duran, 2012).

Due to the natural idealization of particle interaction controlled by their contact and defining their motion explicitly, many scholars have used the discrete element method (DEM) to simulate the collapse process of granular materials (Staron and Hinch, 2005; Zenit, 2005; Lacaze et al., 2008; Lo et al., 2009; Girolami et al., 2012; Soundararajan, 2015; Utili et al., 2015). In these studies the effect of initial porosity (corresponding to soil density) was neglected. More recently, Kermani et al. (2015) and Soundararajan (2015) simulated the effect of the initial void ratio on a 3D asymmetric collapse with different aspect ratios and revealed that a lower value of initial porosity leads to a higher final deposition height, i.e. consistent with the experimental records of Daerr and Douady (1999). Although the simulation results of the above studies are roughly in agreement with the indoor physical experiments, they did not consider the influence of particle shape. Besides, due to computational inefficiency, the number of particles in most DEM simulations is limited and far from the actual physical model, and extension of the DEM to real scale problems remains questionable.

Unlike DEM modelling, the finite element method (FEM) benefits from high computational efficiency and is based on the principles of continuum mechanics, which can be improved by implementing an appropriate constitutive model. To overcome the severe grid distortion by reason of large deformation in conventional FEM calculations, various meshless methods have been developed in recent years (Ren et al., 2015; Fan et al., 2016; Fan and Li, 2017; Gu et al., 2019; Qiu et al., 2019; Hu et al., 2020). Meshless FEM simulations of granular column collapse have been conducted using the arbitrary Lagrangian-Eulerian (ALE) approach (Crosta et al., 2009), particle finite element method (PFEM) (Zhang et al., 2014; Dávalos et al., 2015), material point method (MPM) (Mast et al., 2015), and smoothed particle hydrodynamics (SPH) method (Bui et al., 2008; Nguyen et al., 2017). Among these meshless approaches, the SPH method does not require the use of any pre-defined meshes that provide nodal connection information, but rather effectively approximates functions based on a set of particles. Whereas in other meshless methods the nodes are used only as interpolation points, the particles in the SPH method have material properties, such as mass and density, and move in response to internal interactions and external forces. Note that the constitutive models used in previous studies mostly adopted the Mohr-Coulomb or Drucker-Prager criteria and are not appropriate for describing the state-dependent behaviour of soils. In addition, the influence of particle shape on granular collapse could not be considered in those studies. Numerical simulations considering mesh-free methods and state-dependent advanced constitutive models are seldom seen in the literature (Yin et al., 2018a). Furthermore, collapse simulations using the SPH method to consider the influence of particle shape are still not available.

For these reasons, in this study a numerical approach based on a meshless FEM and critical state soil mechanics was used to investigate the characteristics of granular collapse. A simple critical state-based model (named SIMSAND) accounting for soil density effect was adopted and combined with the SPH method for considering large deformation. A series of benchmark simulations of axisymmetric collapse using DEM were first conducted and then used to validate the performance of the adopted modelling strategy. For the DEM benchmark simulations, three different particle shapes, namely spherical, tetrahedral, and elongated, were chosen to study

the effect of particle shape on column axisymmetric collapse. The related model parameters were calibrated from triaxial tests using an optimization-based parameter identification method. Then the granular collapse with different particle shapes was investigated by the proposed approach. In addition to the effect of particle shapes, columns with different initial void ratios and aspect ratios were also simulated to evaluate the effects of soil density and sample geometry on the final deposit configuration of column collapse.

2 Numerical model

2.1 SPH method

To consider the large deformation in this study, the SPH method integrated in the FEM code ABAQUS/Explicit was adopted. This method was developed by Gingold and Monaghan (1977), initially for calculating astrophysical problems. Further developments extended SPH to solid mechanics. Brief introductions to SPH method can be found in the literature (Jin Z et al., 2019a, 2019b).

2.2 Critical state-based sand model SIMSAND

The SIMSAND model was developed based on the Mohr-Coulomb model by implementing the critical state concept with non-linear elasticity, non-linear plastic hardening, and a simplified 3D strength criterion. A comprehensive description of this model can be found in (Jin et al., 2016b, 2017a). The model parameters with their definitions are summarized in Table 1. The calibration of the model parameters can be carried out using a straightforward method (Wu et al., 2017) or using optimization methods (Jin et al., 2016a; Yin et al., 2018b). The adopted SIMSAND model was implemented into ABAQUS/Explicit as a user-defined material model via the user material subroutine VUMAT. A flow chart of the explicit analysis is presented in Fig. 1.

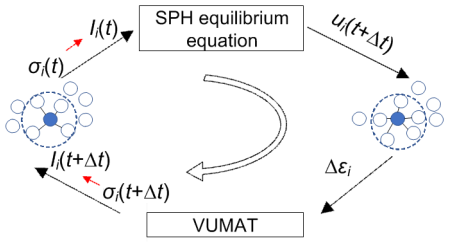

Fig. 1 Flow chart of explicit analysis of SIMSAND model combined with SPH method in ABAQUS code
I_i, σ_i, and u_i are the nodal internal force, cell stress, and nodal displacement at the ith calculation step, respectively; t is the calculation time; $\Delta\varepsilon_i$ is the cell strain increment

3 Simulation of column collapse using DEM

In this study, to validate the performance of the adopted modelling strategy, i.e. the critical state-based constitutive model SIMSAND combined with the meshless method SPH, a series of DEM simulations were first conducted to provide benchmark data. The 3D discrete element tool PFC3D was used to perform a numerical simulation. Fig. 2 shows a profile schematic diagram of the column collapse model: four initial aspect ratios (a=0.5, 1.0, 2.0, 4.0, respectively) were taken into account, the radius r_0 of each column was kept constant and set as 50 mm, and the height

Table 1 Constitutive model parameters used in the simulation of column collapse

Parameter	Definition	Value		
		SS	TS	ES
K_0	Referential bulk modulus (dimensionless)	100	100	100
υ	Poisson's ratio	0.2	0.2	0.2
n	Elastic constant controlling nonlinear stiffness	0.51	0.51	0.51
Φ (°)	Critical state friction angle	18.5	24.0	26.0
e_{ref}	Initial critical state void ratio	0.76	0.76	0.74
λ	Constant controlling the nonlinearity of CSL	0.04	0.04	0.04
ξ	Constant controlling the nonlinearity of CSL	0.3	0.3	0.3
A_{d}	Constant of magnitude of the stress-dilatancy	1.0	1.0	1.0
k_{p}	Plastic modulus related constant	0.0015	0.0015	0.0015
n_{p}	Inter-locking related peak strength parameter	3.3	3.3	3.3
n_{d}	Inter-locking related phase transformation parameter	1.0	1.0	1.0

SS: spherical shape; TS: tetrahedral shape; ES: elongated shape; CSL: critical state line

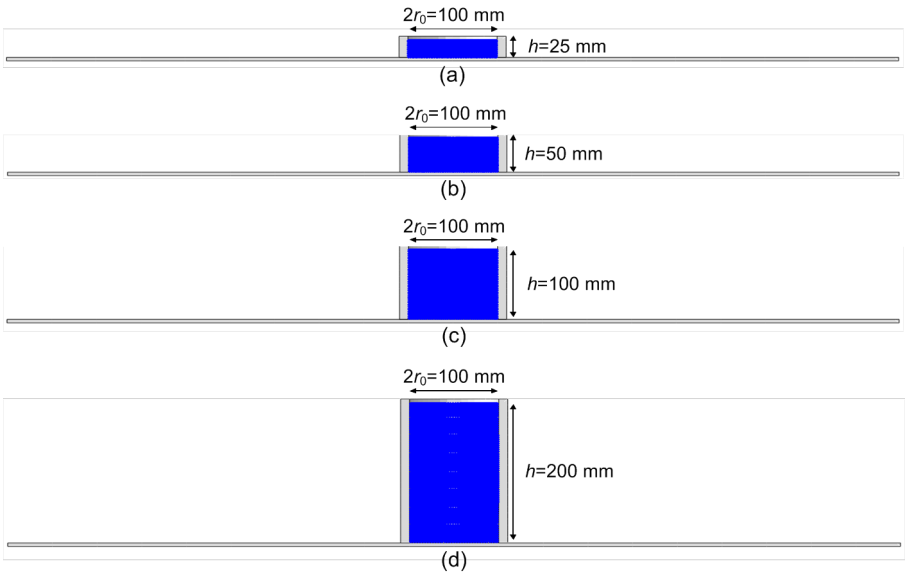

Fig. 2 Profile schematic diagram of four cases (a)–(d) with different aspect ratios *a*

h varied with the aspect ratio. The hollow cylinder pipe containing the granular samples, and the flat sheet at the bottom, were modelled as rigid bodies.

To study the effect of particle shape on axisymmetric collapse, three particle shapes were used: SS, TS, and ES. In addition to the shape of the particles, columns of two different densities were studied simultaneously, namely "dense" and "loose" columns. Dense and loose specimens were investigated by adjusting the initial friction coefficient during the particle settling process. For the "dense" column, the initial friction coefficient of the particles was 0.0. The rolling resistance was assumed to be zero for the interaction between the particles. Under the action of gravity, the particles can fall and deposit more easily, thereby generating a dense column. For the "loose" column, the initial coefficient of friction of the particles was 1.0, making the resulting particle structure loose. Table 2 gives the relevant parameters of the 24 kinds of column samples simulated in this study. For the discrete element calculation domain, the contact between particles was described by a linear contact model, and its related parameters are listed in Table 3.

After obtaining a standard cylindrical specimen, the simulation of the collapse process of the granular material can be achieved by giving a certain vertical upward velocity of the constrained sidewalls. Based on the model tests conducted by Lajeunesse et al. (2004), the lifting speed of the restraining wall was set to 1.6 m/s.

Table 2 Related parameters of DEM simulations for all granular samples

Aspect ratio, a	Particle shape	Relative density	Sample radius, r_0 (mm)	Sample height, h (mm)	Void ratio, e_0	Particle number
0.5	SS	Dense	50	25	0.369	9187
	SS	Loose			0.454	7984
	TS	Dense			0.311	10051
	TS	Loose			0.464	7830
	ES	Dense			0.315	9967
	ES	Loose			0.477	7645
1.0	SS	Dense	50	50	0.367	18474
	SS	Loose			0.451	16062
	TS	Dense			0.308	20254
	TS	Loose			0.467	15617
	ES	Dense			0.310	20124
	ES	Loose			0.462	15617
2.0	SS	Dense	50	100	0.366	36958
	SS	Loose			0.450	32167
	TS	Dense			0.303	40711
	TS	Loose			0.449	32155
	ES	Dense			0.307	40436
	ES	Loose			0.452	32029
4.0	SS	Dense	50	200	0.380	72308
	SS	Loose			0.444	64905
	TS	Dense			0.299	81847
	TS	Loose			0.443	65030
	ES	Dense			0.304	81173
	ES	Loose			0.441	65294

Table 3 Inter-particle properties used in DEM simulations

Parameter	Value
Density, ρ_s (kg/m^3)	2500
Friction coefficient, μ (particle-particle)	0.5
Friction coefficient, μ (particle-wall)	0.0, 0.5
Normal contact stiffness, k_n (N/m)	1.0×10^7
Tangential contact stiffness, k_s (N/m)	6.0×10^6

4 Simulations of column collapse using the SPH with SIMSAND model

4.1 Numerical model

To validate the SIMSAND model and the adopted numerical integration scheme, the DEM axisymmetric column collapse simulations presented in the previous section were followed. The same geometric size was adopted. The PFC3D calculation domain was replaced with SPH particles. For the SPH domain, a cell size of 0.001 m was estimated by checking mesh-dependency. The outer restraining wall and the plate at the bottom were simulated as rigid bodies. The inner restraining wall was assumed to be smooth and the friction between particles and the inner surface of the restraining wall negligible.

A gravity field was specified to the entire model. Once the restraining wall was removed, the specimen began to collapse under the influence of gravity, and the particles expanded outward along the base plate, gradually ceasing to move and stabilizing as energy was dissipated. While performing the collapse simulation calculations, the height of the specimen at the current moment and the distance the particles ran out were recorded simultaneously to analyze the dynamic process of collapse.

4.2 Calibration of model parameters

A series of drained triaxial tests by DEM were conducted to obtain the parameters of the SIMSAND model. For the three kinds of particle shape, a total of six tests, including three on dense samples and three on loose samples, were carried out under different confining pressures (10, 5, and 2 kPa). The model parameters can be determined through optimization-based or Bayesian-based parameter identification procedures (Jin YF et al., 2017b, 2018, 2019a, 2019b; Yin et al., 2017, 2018b; Jin and Yin, 2020). The parameters with more importance were put into the optimization procedure and then optimized, as summarized in Table 4. The detailed description and comparison between numerical simulation results of SIMSAND model and DEM triaxial test are summarized in related study (Lu et al., 2021).

4.3 Validation with experimental results

To first validate the SPH-SIMSAND method, the rectangular channel soil collapse test (Bui et al., 2008) was simulated. Comprehensive simulation details can be obtained from Yin et al. (2018a). Here, we present only the final comparative results (Fig. 3).

The simulation results agree well with the experimental results for considering spherical particles. The results demonstrate that the proposed SPH-SIMSAND method is effective for simulating the soil collapse.

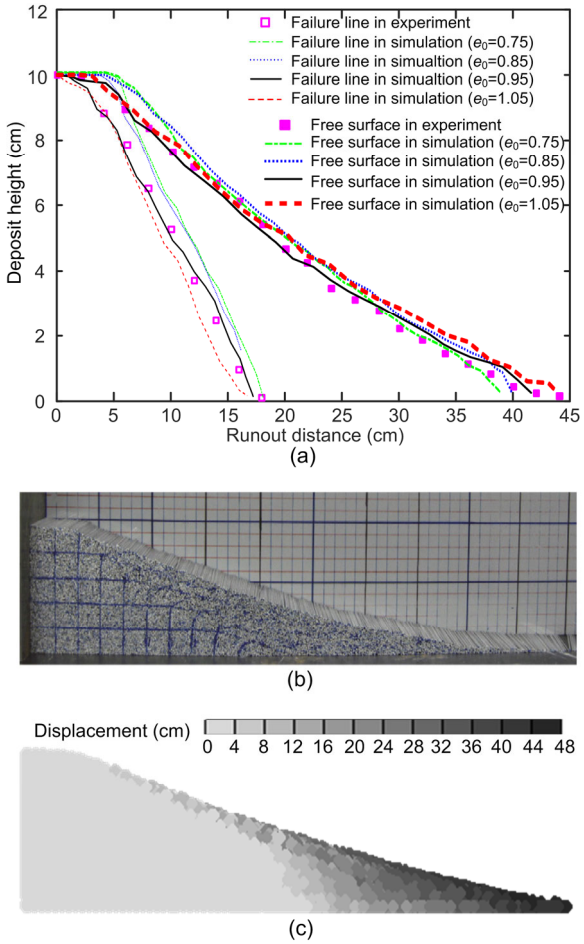

Fig. 3 Simulation results of column collapse

(a) Final free surfaces and failure lines for various initial void ratios e_0=0.75, 0.85, 0.95, 1.05; (b) Final deformed column in experiment; (c) Final deformed column by simulation with e_0=0.95

Table 4 Parameters of the SIMSAND model for simulating all samples

Sample	e_{ref}	λ	ξ	Φ	k_p	A_d	n_p	n_d
SS	0.76	0.04	0.3	18.5	0.0015	1.0	3.3	1.0
TS	0.76	0.04	0.3	24.0	0.0015	1.0	3.3	1.0
ES	0.74	0.04	0.3	26.0	0.0015	1.0	3.3	1.0

5 Axisymmetric collapse simulation results and discussion

There is increasing interest in the extent of damage and the mechanisms involved in natural disasters such as landslides and avalanches. Therefore, the simulation results of the collapse of cylindrical specimens of granular materials have focused on the analysis of the collapse mechanism and description of the final morphology. During the simulation, the height of the specimen in the current collapsed state and the maximum runout distance of the particles were recorded at regular intervals. When the height of the specimen at two adjacent recording moments no longer changed, a steady state was considered to have been reached and the collapse process was complete.

The displacement field of the column (aspect ratio a=2.0) when collapsed to a stable state was recorded for both the DEM and SPH cases, and for each of the three different particle shapes (Fig. 4). The height of each of the three specimens was less than their initial height due to the collapse of the upper part of the specimen. In addition, in the central region of the specimen, the magnitude of the displacement of the particles was close to zero, which indicates that these particles did not move during the collapse process. This region is referred to as the non-disturbed zone. In 3D space, the non-disturbed region is approximated by a cone. According to experience, the cylindrical specimen generated by spherical particles (Fig. 5a) will have the largest runout distance. The runout distances of the columns composed of regular tetrahedral (Fig. 5b) or elongated particles (Fig. 5c) were relatively small, and the final deposit configurations were similar, indicating that the mechanical properties of these two particle morphologies were

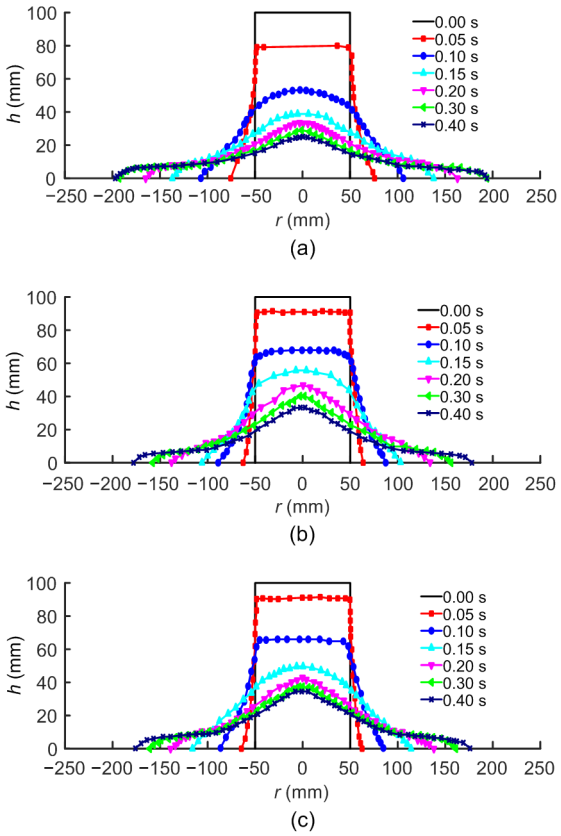

Fig. 5 Outlines of collapse patterns at different times simulated by SPH method
(a) Spherical (SS); (b) Tetrahedral (TS); (c) Elongated (ES)

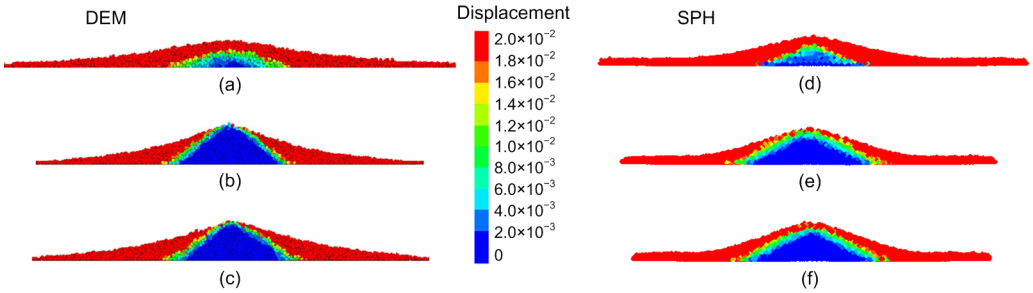

Fig. 4 Displacement field of final morphology for different particle shapes by DEM and SPH method
(a–c) DEM cases including spherical (SS) (a), tetrahedral (TS) (b), and elongated (ES) (c); (d–f) SPH cases including spherical (SS) (d), tetrahedral (TS) (e), and elongated (ES) (f)

relatively close. The results obtained by the SPH method also reflected the main characteristics of the axisymmetric collapse described above.

During the collapse simulation, the current collapse pattern was recorded at regular intervals, and the final outline of the collapse at each moment could be obtained. Figs. 5 and 6 show diagrams of the continuous change of the outline during the collapse of the three specimens simulated by the DEM and SPH method, respectively. For the sample composed of spherical particles, in the initial stage of collapse (Fig. 6a), the upper part of the pattern remained approximately horizontal, mainly because the flow of the lower particles caused the pattern to move downward as a whole, and the final deposit shape was relatively flat. For the specimens composed of tetrahedral or elongated particles, the outer edge particles at the top of the sample began to flow, and the upper part was no longer horizontal until the collapse was completed, and a spire was finally formed. The collapse of tetrahedral and elongated particles appeared to be slower than that of the spherical particles (Fig. 6): the height of the former two specimens was greater than that of the spherical particles at the same moment of collapse. Essentially the same collapse phenomena could also be observed in the cases simulated with the SPH method (Fig. 5).

Fig. 7 presents the relationship between the normalized height h/h_0 and time during the collapse, where h_0 is the initial height of sand sample. The collapse process of cylindrical specimens of granular material can be divided into three stages:

1. Initial collapse phase. This phase lasts about 0.05 s, during which the height of the specimen is slowly reduced.

2. Collapse damage phase. The time period of this phase is roughly 0.05–0.40 s, during which the rate of particle movement increases dramatically and the height of the specimen decreases rapidly.

3. Stabilization phase. At about 0.40 s, the collapse process is almost complete, the particles enter a stable state, and the height of the sample does not change.

In addition, the collapse process and final morphology of tetrahedral and elongated particles were generally consistent. Spherical particles had the fastest collapse process and the lowest final collapse height. Although there were some minor differences, the DEM simulation results and the SPH cases basically reproduced the same collapse process.

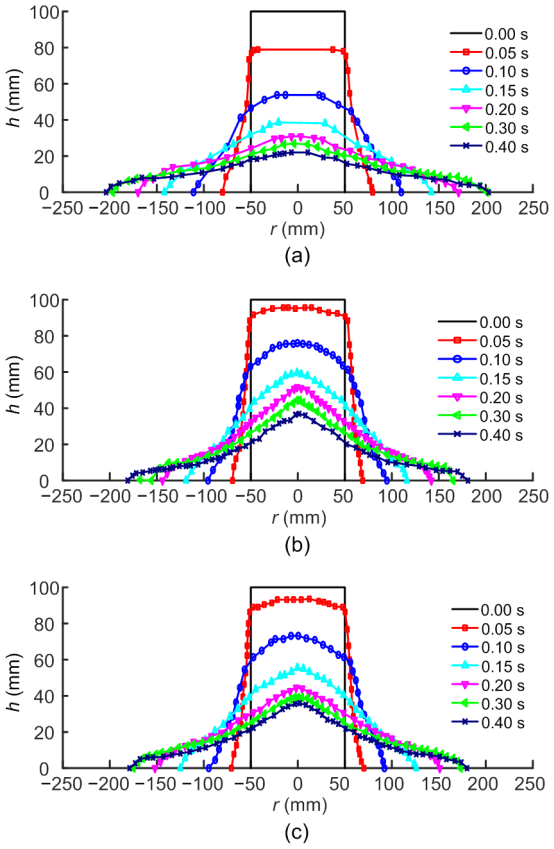

Fig. 6 Outlines of collapse patterns at different times simulated by DEM

(a) Spherical (SS); (b) Tetrahedral (TS); (c) Elongated (ES)

For the collapse test of the cylindrical sample of granular material, the final collapse height h_f and the running distance r_f were the main indicators to describe the collapsed shape. Figs. 8 and 9 summarize the relationship between the normalized final collapse height h_f/r_0 and the normalized final runout distance $(r_f-r_0)/r_0$ versus different initial aspect ratios a, simulated by DEM and SPH method, respectively. The model test results of Lajeunesse et al. (2004) and Lube et al. (2004) are also plotted in these graphs. It is clear that the simulation results of tetrahedral and elongated particles fall on the empirical curve, which is in good agreement with the indoor test results. However, the spherical particle results present an obvious deviation from the empirical curve. One possible reason is that the spherical particle shape can barely constrain the rotation of the particles, resulting

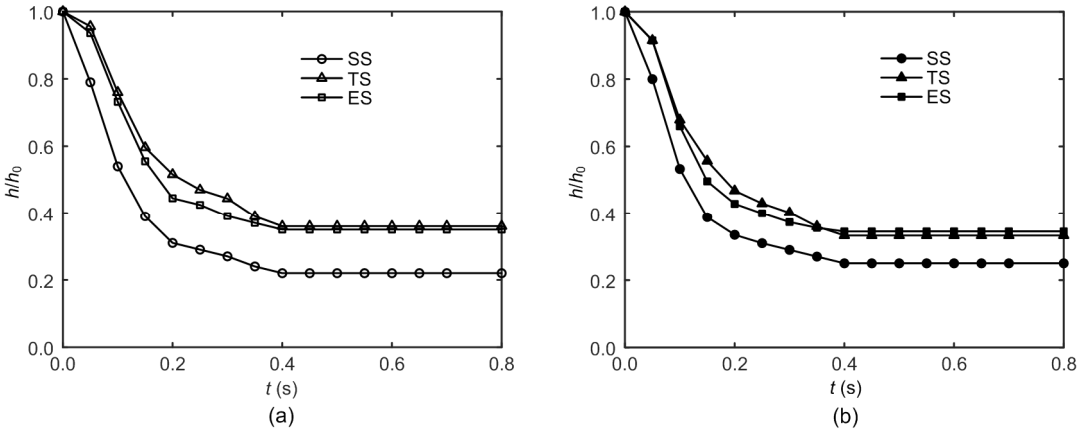

Fig. 7 Normalized collapse height h/h_0 versus time
(a) DEM simulations; (b) SPH simulations

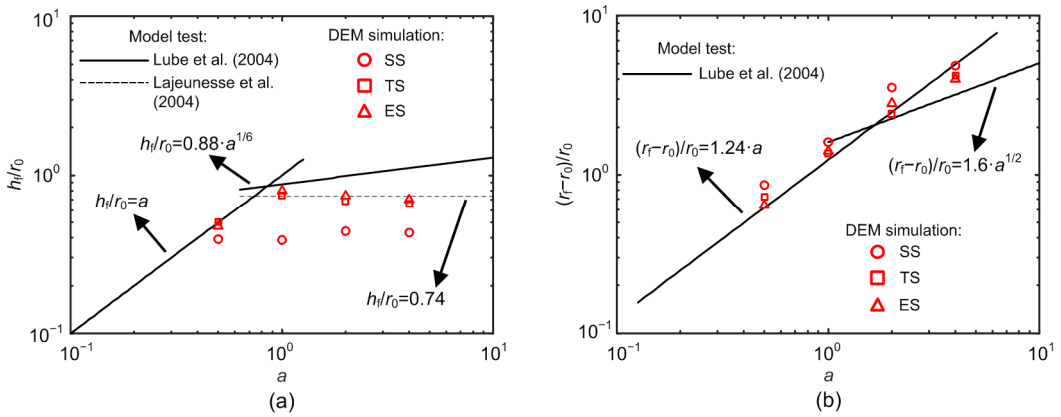

Fig. 8 Comparison between the DEM simulations and the best-fitting equations of Lajeunesse et al. (2004) and Lube et al. (2004) for different aspect ratios
(a) Normalized final deposit height; (b) Normalized final runout distance

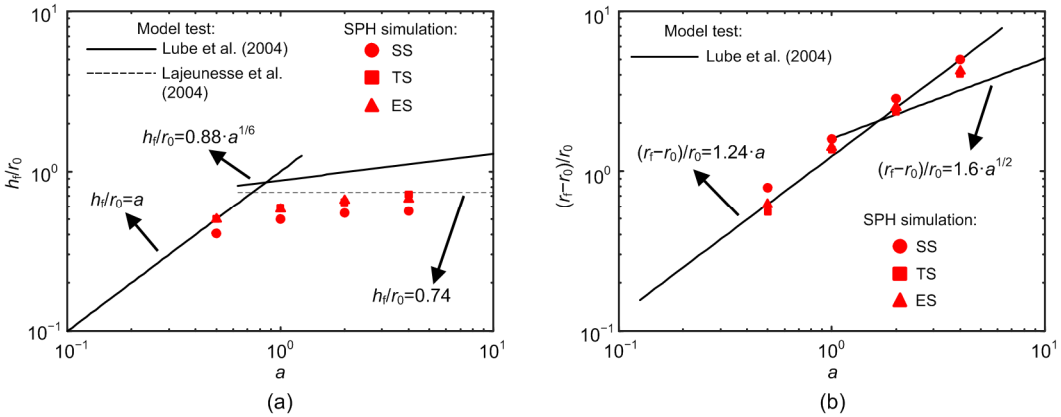

Fig. 9 Comparison between the SPH simulations and the best-fitting equations of Lajeunesse et al. (2004) and Lube et al. (2004) for different aspect ratios
(a) Normalized final deposit height; (b) Normalized final runout distance

in a small final collapse height h_f and a large runout distance r_f. A comparison of the simulation results of tetrahedral and elongated particles shows that the final collapse heights and runout distances were

similar, indicating that the two particle shapes were equally effective in reducing particle rotation. This can also be explained by the results of the triaxial test simulations: the critical friction angles of these two shapes were similar, 24.0° and 26.0°, respectively.

To investigate the effect of the initial void ratio and aspect ratio on the collapse of axisymmetric column specimens, a total of 24 groups were simulated, representing four aspect ratios (a=0.5, 1.0, 2.0, 4.0), three kinds of particle shapes (spherical (SS), tetrahedral (TS), elongated (ES)), and two initial void ratios (loose and dense). Fig. 10 summarizes the displacement field of the final deposit pattern for all these specimens simulated with the SPH method. When the aspect ratio a=0.5, the undisturbed area was trapezoidal, indicating that collapse occurred only in a certain area around the specimen, while the central area was almost unaffected. When the aspect ratio a=1.0, 2.0, or 4.0, the undisturbed area was triangular. In addition, for a=1.0 and 2.0, the undisturbed region reached the top, while for the case of a=4.0, the undisturbed region was covered with a large number of disturbed particles. One reasonable explanation is that for samples with a relatively small aspect ratio a (not including a=0.5), the undisturbed area inside the sample can be seen as a fixed conical boundary during the collapse of the sample, and the surrounding particles collapse under gravity. After encountering the "boundary" of the undisturbed area, it will continue to collapse and spread to the surrounding area until finally stabilized. For specimens with a relatively large aspect ratio a, due to the large number of disturbed collapsed particles, the collapsed particles gradually stabilize and accumulate, and some particles stop above the undisturbed zone, resulting in the phenomenon described above. At the same time, since the top particles of specimens with a larger height to diameter ratio a (a=4.0) store more gravitational potential energy, which is gradually converted into kinetic energy during the collapse process, the collapse runs out over a longer distance and over a larger collapse area.

Comparative analysis of the deposit morphology and the shape of the undisturbed area after the collapse of the loose and dense cylindrical specimens shows that the density of the specimen had a significant effect on the collapse: in general, the loose specimens were more likely to collapse, and the final collapse height was less than that of the dense sample; correspondingly, the size of the undisturbed area of the loose sample was smaller than that of the dense one.

6 Conclusions

In this paper, based on the soil model SIMSAND considering critical state and the SPH approach, a highly efficient and accurate approach for numerically simulating axisymmetric column collapse was proposed. Using benchmarks obtained by DEM simulation as a reference group, a total of 24 specimens were simulated with different initial conditions: four different aspect ratios (a=0.5, 1.0, 2.0, 4.0), three different particle shapes (spherical, regular tetrahedral, and elongated), and two different initial densities (dense and loose). The results of final deposit morphology, runout distance, collapse height, and undisturbed area were analysed.

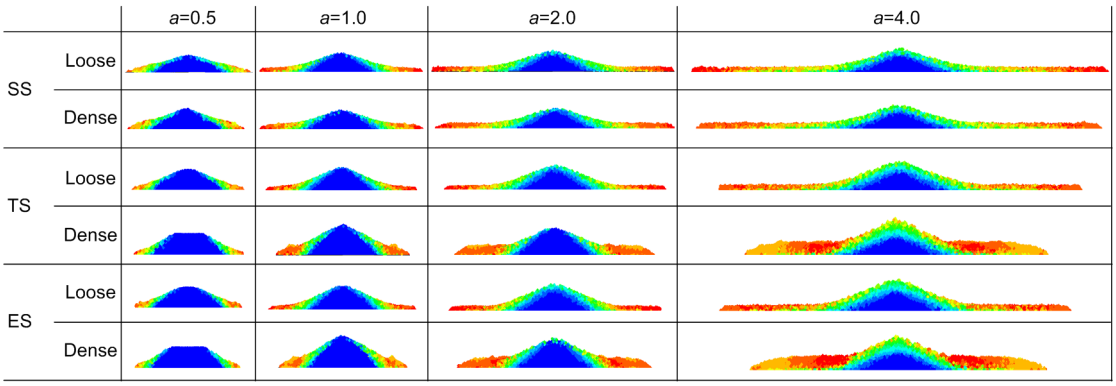

Fig. 10 Displacement field of final deposit morphology for specimens considering different initial void ratios, aspect ratios, and particle shapes, simulated by SPH method

Comparisons proved that the numerical approach adopted made it possible to reproduce qualitatively and quantitatively the main characteristics of the collapse of the columns, i.e. the runout distance, collapse height, and final deposit configurations. In particular, the numerical simulation results showed that the particle shape and initial density had a significant effect on the axisymmetric collapse. For the specimens composed of tetrahedral or elongated particles, the simulation results were in good agreement with laboratory test data. However, the results for those composed of spherical particles showed an obvious deviation. This indicated that the physical characteristics of the irregular particle shapes (tetrahedral and elongated) were closer to those of granular materials used in model tests than were the spherical particles. In addition, these two particle shapes had similar restraining effects on particle rotation based on their similar numerical simulation results. Compared with the "loose" column, the "dense" column had a shorter runout distance and a larger undisturbed area.

The combination of the SPH method and SIMSAND model is acceptable for reproducing axisymmetric collapse while considering the effects of particle shapes and soil densities. This newly proposed strategy also has a higher computational efficiency than the DEM method, while guaranteeing computational accuracy. Overall, this numerical approach can be an effective numerical tool and can be applied for further analysis of real scale engineering problems.

Acknowledgements

The numerical simulations in this paper were supported by the Center for Computational Science and Engineering, Southern University of Science and Technology, China.

Contributors

Zhuang JIN designed the research, processed the corresponding data, and wrote the first draft of the manuscript. Zhao LU helped to organize the manuscript. Zhao LU and Yi YANG revised and edited the final version.

Conflict of interest

Zhuang JIN, Zhao LU, and Yi YANG declare that they have no conflict of interest.

References

Balmforth NJ, Kerswell RR, 2005. Granular collapse in two dimensions. *Journal of Fluid Mechanics*, 538:399-428. https://doi.org/10.1017/S0022112005005537

Bui HH, Fukagawa R, Sako K, et al., 2008. Lagrangian meshfree particles method (SPH) for large deformation and failure flows of geomaterial using elastic-plastic soil constitutive model. *International Journal for Numerical and Analytical Methods in Geomechanics*, 32(12):1537-1570. https://doi.org/10.1002/nag.688

Crosta GB, Imposimato S, Roddeman D, 2009. Numerical modeling of 2-D granular step collapse on erodible and nonerodible surface. *Journal of Geophysical Research*, 114(F3):F03020. https://doi.org/10.1029/2008JF001186

Daerr A, Douady S, 1999. Sensitivity of granular surface flows to preparation. *EPL (Europhysics Letters)*, 47(3):324-330. https://doi.org/10.1209/epl/i1999-00392-7

Dávalos C, Cante J, Hernández JA, et al., 2015. On the numerical modeling of granular material flows via the particle finite element method (PFEM). *International Journal of Solids and Structures*, 71:99-125. https://doi.org/10.1016/j.ijsolstr.2015.06.013

Duran J, 2012. Sands, Powders, and Grains: an Introduction to the Physics of Granular Materials. Springer Science & Business Media, New York, USA. https://doi.org/10.1007/978-1-4612-0499-2

Fan HF, Li SF, 2017. A peridynamics-SPH modeling and simulation of blast fragmentation of soil under buried explosive loads. *Computer Methods in Applied Mechanics and Engineering*, 318:349-381. https://doi.org/10.1016/j.cma.2017.01.026

Fan HF, Bergel GL, Li SF, 2016. A hybrid peridynamics–SPH simulation of soil fragmentation by blast loads of buried explosive. *International Journal of Impact Engineering*, 87:14-27. https://doi.org/10.1016/j.ijimpeng.2015.08.006

Fern EJ, Soga K, 2016. The role of constitutive models in MPM simulations of granular column collapses. *Acta Geotechnica*, 11(3):659-678. https://doi.org/10.1007/s11440-016-0436-x

Gingold RA, Monaghan JJ, 1977. Smoothed particle hydrodynamics: theory and application to non-spherical stars. *Monthly Notices of the Royal Astronomical Society*, 181(3):375-389. https://doi.org/10.1093/mnras/181.3.375

Girolami L, Hergault V, Vinay G, et al., 2012. A three-dimensional discrete-grain model for the simulation of dam-break rectangular collapses: comparison between numerical results and experiments. *Granular Matter*, 14(3):381-392. https://doi.org/10.1007/s10035-012-0342-3

Gu Q, Wang L, Huang SR, 2019. Integration of peridynamic theory and OpenSees for solving problems in civil engineering. *Computer Modeling in Engineering & Sciences*, 120(3):471-489.

https://doi.org/10.32604/cmes.2019.05757

Hu CB, Wang L, Ling DS, et al., 2020. Experimental and numerical investigation on the tensile fracture of compacted clay. *Computer Modeling in Engineering & Sciences*, 123(1):283-307. https://doi.org/10.32604/cmes.2020.07842

Jin YF, Yin ZY, 2020. Enhancement of backtracking search algorithm for identifying soil parameters. *International Journal for Numerical and Analytical Methods in Geomechanics*, 44(9):1239-1261. https://doi.org/10.1002/nag.3059

Jin YF, Yin ZY, Shen SL, et al., 2016a. Investigation into MOGA for identifying parameters of a critical-state-based sand model and parameters correlation by factor analysis. *Acta Geotechnica*, 11(5):1131-1145. https://doi.org/10.1007/s11440-015-0425-5

Jin YF, Yin ZY, Shen SL, et al., 2016b. Selection of sand models and identification of parameters using an enhanced genetic algorithm. *International Journal for Numerical and Analytical Methods in Geomechanics*, 40(8): 1219-1240. https://doi.org/10.1002/nag.2487

Jin YF, Wu ZX, Yin ZY, et al., 2017a. Estimation of critical state-related formula in advanced constitutive modeling of granular material. *Acta Geotechnica*, 12(6):1329-1351. https://doi.org/10.1007/s11440-017-0586-5

Jin YF, Yin ZY, Shen SL, et al., 2017b. A new hybrid real-coded genetic algorithm and its application to parameters identification of soils. *Inverse Problems in Science and Engineering*, 25(9):1343-1366. https://doi.org/10.1080/17415977.2016.1259315

Jin YF, Yin ZY, Wu ZX, et al., 2018. Identifying parameters of easily crushable sand and application to offshore pile driving. *Ocean Engineering*, 154:416-429. https://doi.org/10.1016/j.oceaneng.2018.01.023

Jin YF, Yin ZY, Zhou WH, et al., 2019a. Identifying parameters of advanced soil models using an enhanced transitional Markov chain Monte Carlo method. *Acta Geotechnica*, 14(6):1925-1947. https://doi.org/10.1007/s11440-019-00847-1

Jin YF, Yin ZY, Zhou WH, et al., 2019b. Multi-objective optimization-based updating of predictions during excavation. *Engineering Applications of Artificial Intelligence*, 78:102-123. https://doi.org/10.1016/j.engappai.2018.11.002

Jin YF, Yuan WH, Yin ZY, et al., 2020. An edge-based strain smoothing particle finite element method for large deformation problems in geotechnical engineering. *International Journal for Numerical and Analytical Methods in Geomechanics*, 44(7):923-941. https://doi.org/10.1002/nag.3016

Jin Z, Yin ZY, Kotronis P, et al., 2019a. Advanced numerical modelling of caisson foundations in sand to investigate the failure envelope in the *H-M-V* space. *Ocean Engineering*, 190:106394. https://doi.org/10.1016/j.oceaneng.2019.106394

Jin Z, Yin ZY, Kotronis P, et al., 2019b. Numerical investigation on evolving failure of caisson foundation in sand using the combined Lagrangian-SPH method. *Marine Georesources & Geotechnology*, 37(1):23-35. https://doi.org/10.1080/1064119X.2018.1425311

Kermani E, Qiu T, Li TB, 2015. Simulation of collapse of granular columns using the discrete element method. *International Journal of Geomechanics*, 15(6):04015004. https://doi.org/10.1061/(ASCE)GM.1943-5622.0000467

Lacaze L, Phillips JC, Kerswell RR, 2008. Planar collapse of a granular column: experiments and discrete element simulations. *Physics of Fluids*, 20(6):063302. https://doi.org/10.1063/1.2929375

Lajeunesse E, Mangeney-Castelnau A, Vilotte JP, 2004. Spreading of a granular mass on a horizontal plane. *Physics of Fluids*, 16(7):2371-2381. https://doi.org/10.1063/1.1736611

Lajeunesse E, Monnier JB, Homsy GM, 2005. Granular slumping on a horizontal surface. *Physics of Fluids*, 17(10):103302. https://doi.org/10.1063/1.2087687

Lo CY, Bolton M, Cheng YP, 2009. Discrete element simulation of granular column collapse. *AIP Conference Proceedings*, 1145(1):627-630. https://doi.org/10.1063/1.3180004

Lu Z, Jin Z, Kotronis P, 2021. Numerical analysis of slope collapse using SPH and the SIMSAND critical state model. *Journal of Rock Mechanics and Geotechnical Engineering*, in press. https://doi.org/10.1016/j.jrmge.2021.03.009

Lube G, Huppert HE, Sparks RSJ, et al., 2004. Axisymmetric collapses of granular columns. *Journal of Fluid Mechanics*, 508:175-199. https://doi.org/10.1017/S0022112004009036

Lube G, Huppert HE, Sparks RSJ, et al., 2005. Collapses of two-dimensional granular columns. *Physical Review E*, 72(4):041301. https://doi.org/10.1103/PhysRevE.72.041301

Lube G, Huppert HE, Sparks RSJ, et al., 2007. Static and flowing regions in granular collapses down channels. *Physics of Fluids*, 19(4):043301. https://doi.org/10.1063/1.2712431

Mast CM, Arduino P, Mackenzie-Helnwein P, et al., 2015. Simulating granular column collapse using the material point method. *Acta Geotechnica*, 10(1):101-116. https://doi.org/10.1007/s11440-014-0309-0

Nguyen CT, Nguyen CT, Bui HH, et al., 2017. A new SPH-based approach to simulation of granular flows using viscous damping and stress regularisation. *Landslides*, 14(1):69-81. https://doi.org/10.1007/s10346-016-0681-y

Qiu ZJ, Lu JC, Elgamal A, et al., 2019. OpenSees three-dimensional computational modeling of ground-structure systems and liquefaction scenarios. *Computer Modeling in Engineering & Sciences*, 120(3):629-656. https://doi.org/10.32604/cmes.2019.05759

Ren B, Fan HF, Bergel GL, et al., 2015. A peridynamics–SPH coupling approach to simulate soil fragmentation induced by shock waves. *Computational Mechanics*, 55(2):287-302. https://doi.org/10.1007/s00466-014-1101-6

Soundararajan KK, 2015. Multi-scale Multiphase Modelling of Granular Flows. PhD Thesis, University of Cambridge, Cambridge, UK.

Staron L, Hinch EJ, 2005. Study of the collapse of granular columns using two-dimensional discrete-grain simulation. *Journal of Fluid Mechanics*, 545:1-27. https://doi.org/10.1017/S0022112005006415

Utili S, Zhao T, Houlsby GT, 2015. 3D DEM investigation of granular column collapse: evaluation of debris motion and its destructive power. *Engineering Geology*, 186:3-16. https://doi.org/10.1016/j.enggeo.2014.08.018

Wu ZX, Yin ZY, Jin YF, et al., 2017. A straightforward procedure of parameters determination for sand: a bridge from critical state based constitutive modelling to finite element analysis. *European Journal of Environmental and Civil Engineering*, 23(12):1444-1466. https://doi.org/10.1080/19648189.2017.1353442

Wu ZX, Ji H, Han J, et al., 2019. Numerical modelling of granular column collapse using coupled Eulerian–Lagrangian technique with critical state soil model. *Engineering Computations*, 36(7):2480-2504. https://doi.org/10.1108/EC-08-2018-0358

Xiong H, Yin ZY, Nicot F, et al., 2021. A novel multi-scale large deformation approach for modelling of granular collapse. *Acta Geotechnica*, 16:2371-2388. https://doi.org/10.1007/s11440-020-01113-5

Yang J, Yin ZY, Laouafa F, et al., 2019a. Analysis of suffusion in cohesionless soils with randomly distributed porosity and fines content. *Computers and Geotechnics*, 111:157-171. https://doi.org/10.1016/j.compgeo.2019.03.011

Yang J, Yin ZY, Laouafa F, et al., 2019b. Internal erosion in dike-on-foundation modeled by a coupled hydromechanical approach. *International Journal for Numerical and Analytical Methods in Geomechanics*, 43(3):663-683. https://doi.org/10.1002/nag.2877

Yang J, Yin ZY, Laouafa F, et al., 2019c. Modeling coupled erosion and filtration of fine particles in granular media. *Acta Geotechnica*, 14(6):1615-1627. https://doi.org/10.1007/s11440-019-00808-8

Yang J, Yin ZY, Laouafa F, et al., 2020. Hydromechanical modeling of granular soils considering internal erosion. *Canadian Geotechnical Journal*, 57(2):157-172. https://doi.org/10.1139/cgj-2018-0653

Yin ZY, Jin YF, Shen SL, et al., 2017. An efficient optimization method for identifying parameters of soft structured clay by an enhanced genetic algorithm and elastic–viscoplastic model. *Acta Geotechnica*, 12(4):849-867. https://doi.org/10.1007/s11440-016-0486-0

Yin ZY, Jin Z, Kotronis P, et al., 2018a. Novel SPH SIMSAND–based approach for modeling of granular collapse. *International Journal of Geomechanics*, 18(11):04018156. https://doi.org/10.1061/(ASCE)GM.1943-5622.0001255

Yin ZY, Jin YF, Shen JS, et al., 2018b. Optimization techniques for identifying soil parameters in geotechnical engineering: comparative study and enhancement. *International Journal for Numerical and Analytical Methods in Geomechanics*, 42(1):70-94. https://doi.org/10.1002/nag.2714

Yuan WH, Wang B, Zhang W, et al., 2019. Development of an explicit smoothed particle finite element method for geotechnical applications. *Computers and Geotechnics*, 106:42-51. https://doi.org/10.1016/j.compgeo.2018.10.010

Yuan WH, Liu K, Zhang W, et al., 2020. Dynamic modeling of large deformation slope failure using smoothed particle finite element method. *Landslides*, 17(7):1591-1603. https://doi.org/10.1007/s10346-020-01375-w

Zenit R, 2005. Computer simulations of the collapse of a granular column. *Physics of Fluids*, 17(3):031703. https://doi.org/10.1063/1.1862240

Zhang X, Krabbenhoft K, Pedroso DM, et al., 2013. Particle finite element analysis of large deformation and granular flow problems. *Computers and Geotechnics*, 54:133-142. https://doi.org/10.1016/j.compgeo.2013.07.001

Zhang X, Krabbenhoft K, Sheng DC, 2014. Particle finite element analysis of the granular column collapse problem. *Granular Matter*, 16(4):609-619. https://doi.org/10.1007/s10035-014-0505-5

Zhang X, Krabbenhoft K, Sheng DC, et al., 2015. Numerical simulation of a flow-like landslide using the particle finite element method. *Computational Mechanics*, 55(1):167-177. https://doi.org/10.1007/s00466-014-1088-z